Supporting Information for

Fused Carbazole–Coumarin–Ketone Dyes: High Performance and Photobleachable Photoinitiators in Free Radical Photopolymerization for Deep Photocuring under Visible LED Light Irradiation

*Xinyue Guo,[a] Huanv Mao,[b] Chunyan Bao,[b] Decheng Wan[a] and Ming Jin[*a]*

[a] Department of Polymer Materials, School of Materials Science and Engineering, Tongji University, 4800 Caoan Road, Shanghai, 201804, P.R. China

[b] School of Chemistry and Molecular Engineering, East China University of Science & Technology, 130 Meilong Road, Shanghai, 200237, P.R. China

Table of Contents

Experimental

Organic synthesis

Experimental

Absorption and emission spectroscopy

The absorption measurements were carried out with Mapada UV-6300 double beam UV–Vis spectrophotometer. The photolysis measurements were carried out under continuous irradiation at 405 nm with a LED point curing (Uvata, Shanghai). Light intensity: 45 mW cm^{-2}. Steady-state fluorescence spectra are collected from a Hitachi-2700 spectrofluorometer. Emission spectra were spectrally corrected, and fluorescence quantum yields include the correction due to solvent refractive index were determined relative to quinine bisulfate in 0.05 M sulfuric acid ($\Phi_{fl} = 0.52$).[1]

Theoretical calculations

The theoretical calculations were computed based on Density Functional Theory (DFT). The overall computation strategy was defined as follows: After initial AM1 optimization calculations. The theoretical absorption properties of molecular structures were calculated at the TD/CAM-B3LYP/6-31G(d) levels and on basis of the frequency checked geometries calculated at the B3LYP/6-31G(d) level. All calculations were performed using the GAUSSIAN 09 package.

Electron spinning resonance spin trapping (ESR-ST) experiment

ESR-ST experiments were carried out using a Bruker EMX-plus spectrometer (X-band). The radicals were generated when exposed to an LED light source (405 nm) at room temperature under nitrogen and were trapped by phenyl *N-tert*-butylnitrone (PBN) in *tert*-butylbene.[2]

Photo-DSC

Photo-DSC measurement was carried out by DSC 500C (Yanjin, Shanghai) equipped with a LED point curing (Uvata, Shanghai), of which the wavelength is 405 nm, 425 nm, 450 nm and 475 nm. Light intensity: 45 mW cm^{-2}. A uniform UV light intensity (checked by the integrating sphere (Ocean Optics)) is delivered across the DSC cell to the sample and reference pans. An approximately 0.90 mg sample mixture was placed in the aluminum crucible, and completely cover the sample with a PET film, at the same time the reference crucible is empty. By integrating the area under the exothermic peak, the conversion or reaction degree of vinyl (C) can be obtained as follows:

$$C = \Delta H_t / \Delta H^{\text{theory}}_0 \tag{1}$$

Where ΔH_t is the reaction heat that evolved at time t and $\Delta H^{\text{theory}}_0$ is the theoretical heat for complete conversion. $\Delta H^{\text{theory}}_a$ is 86 kJ mol^{-1} for an acrylate double bond,[3] and the total $\Delta H^{\text{theory}}_0$ for photo-curing formulation per mg was calculated as eq. (2), here n was the number of acrylate double bond for per monomer, $\%_m$ was the proportion of monomer in formulation and M_m the molecular weight of monomer:

$$\Delta H^{\text{theory}}_0 = \frac{n \cdot \%_m \cdot \Delta H^{\text{theory}}_a}{M_m} \tag{2}$$

The test was repeated three times in parallel, and the average conversion value of the three experiments was taken.

Cytocompatibility

For cytocompatibility testing, L929-mCherry cells were cultivated in Dulbecco's modified Eagle medium (DMEM) supplemented with 10% fetal bovine serum (FBS), penicillin (100 units mL^{-1}), and streptomycin (100 μg mL^{-1}) at an incubator in humid atmosphere with 5% carbon dioxide at 37 ℃. The

medium was refreshed every second day. After 3 days, cells were harvested by 0.25% (v/v) trypsin solution and the obtained cell suspensions were re–suspended in fresh medium. For cytotoxicity testing, cells were seeded in 96-well plates at an initial density of 10000 cells per well in 100 μL of above DMEM culture medium. After coculture overnight for cell attachment, the culture medium was replaced with 100 μL fresh medium containing different concentrations of photointiator CCK–Tol in 1 μL DMSO (0.10, 0.05, 0.025, 0.0125, 0.00625 and 0.003125 mM, final concentrations). After 24 h coculture, the medium in the wells was removed and exchanged twice with fresh medium to remove the residue compounds. Then, 100 μL fresh medium containing CCK-8 reagent (10 μL) was added to each well and the cells were incubated for another 2 h at 37 ºC. Finally, the cytotoxicity was quantified by the absorbance at 450 nm using a m^{4}icroplate reader, and cell viability was expressed as the ratio of the number of viable cells with treatment to that without treatment. Every sample was tested at least 6 repetitions. For comparison, the cytotoxicity of DMSO was also investigated and non–treated cells were used as controls. The cell survival rate is calculated by the following formula from the average of six parallel experiments.

$$\text{Cell viability (\%)} = \frac{A_{\text{experiment}} - A_0}{A_{\text{control}} - A_0} \times 100\% \tag{3}$$

Where $A_{\text{experiment}}$ means the absorbance of the cells treated with photoinitiator, A_{control} means the absorbance of the cells without any treatment, and A_0 means the absorbance of blank sample without cells.

To investigate the cytotoxicity of photoproduct, the CCK–Tol DMSO solutions were irradiated at LED@405 nm (100 mW cm^{-2}) for 15 min. Then, the photoproduct solutions were cocultured with cells for cell viability evaluation. The detailed process was similar as the unirradiated samples.

Confocal microscopy of cell live–dead staining

Cells were seeded in confocal dishes at an initial density of 1.0×10^4 cells per well in 1 mL of culture medium. After overnight incubation, DMEM was then replaced with culture medium containing CCK–Tol or irradiated CCK–Tol at different concentrations (0, 0.025, 0.05 and 0.1 mM, final concentration). After coculture of 24 h, the medium in each well was removed, and the attached cells were gently washed with PBS and stained with a live/dead reagent (calcein-AM/PI) for 0.5 h, where live and dead cells were imaged by fluorescence confocal microscope at excitation wavelengths of 488 nm and 561 nm, respectively. The live cells presented green fluorescence upon 488 nm excitation and the dead cells emitted red fluorescence upon 561 nm excitation.

Organic synthesis

Synthesis of 3-formyl-4-hydroxy carbazole (**1**). Phosphorous oxychloride (4.43 mL, 47.00 mmol) was added dropwise to dry DMF (7.28 mL, 94.01 mmol) at 0–5 °C, and stirred for 30 min maintaining the temperature 0~5 °C. 4-hydroxy carbazole (7.69 g, 42.00 mmol) dissolved in 20 mL DMF was added dropwise within 30 min maintaining temperature between 0 to 5 °C. Stirring was continued for next 20–30 min, reaction mixture was then brought to room temperature and heated at 70–75 °C for 1 h. Completion of reaction was monitored by TLC. The obtained reaction mass poured into crushed ice stirred well and neutralized with sodium bicarbonate. Precipitate obtained was filtered off and dried. The crude product was further purified by silica gel column chromatography (petroleum ether/ethyl acetate = 4: 1) to get hold of 4-hydroxy-*9H*-carbazole-3-carbaldehyde in 52% yield. ^{1}H NMR (400 MHz, Chloroform–*d*): δ 12.42 (s, 1H), 9.88 (s, 1H), 8.37 (d, J = 7.7 Hz, 2H), 7.49 (d, J = 8.4 Hz, 1H), 7.45 (d, J = 3.8 Hz, 3H), 7.34 (dt, J = 8.0, 4.1 Hz, 1H), 7.01 (d, J = 8.4 Hz, 1H).

Synthesis of 3-acetylpyrano[*3,2-c*]carbazole-2(*7H*)-one (**2a**). 4-hydroxy-*9H*-carbazole-3-carbaldehyde (0.80 g, 3.79 mmol) and ethyl acetoacetate (0.59 g, 4.55 mmol) was dissolved in 20 mL ethanol, catalytic amount of piperidine was added to it and refluxed for 2 h, bright yellow crystalline compound separate out. Completion of reaction was monitored by TLC. Reaction mass filtered and crude product obtained was recrystallized from ethanol to get hold of 3-acetylpyrano[3,2-c]carbazole-2(7H)-one in 84% yield. ^{1}H NMR (400 MHz, DMSO-d_6): δ 12.22 (s, 1H), 8.82 (s, 1H), 8.30 (d, J = 7.8 Hz, 1H), 7.88 (d, J = 8.5 Hz, 1H), 7.64 (d, J = 8.1 Hz, 1H), 7.56 – 7.48 (m, 2H), 7.38 (t, J = 7.5 Hz, 1H), 3.35 (s, 3H).

Synthesis of 3-benzoylpyrano[*3,2-c*]carbazole-2(*7H*)-one (**2b**). **2b** was synthesized from ethyl benzoylacetate according to the procedure described as **2a**, with a yield of 82%. ^{1}H NMR (400 MHz,

DMSO-d_6): δ 12.18 (s, 1H), 8.63 (s, 1H), 8.33 (d, J = 7.8 Hz, 1H), 7.94 (d, J = 7.2 Hz, 2H), 7.85 (d, J = 8.5 Hz, 1H), 7.73 – 7.61 (m, 3H), 7.55 (dt, J = 7.9, 3.7 Hz, 6H), 7.37 (t, J = 7.5 Hz, 1H).

Synthesis of 3-(2-methylbenzoyl)pyrano[*3,2-c*]carbazole-2(*7H*)-one (**2c**). **2c** was synthesized from ethyl 3-oxo-3-(*o*-tolyl)propanoate according to the procedure described as **2b**, with a yield of 81%. [^1]H NMR (400 MHz, DMSO-d_6): δ 12.25 (s, 1H), 8.67 (s, 1H), 8.34 (d, J = 7.8 Hz, 1H), 7.90 (d, J = 8.6 Hz, 1H), 7.69 (d, J = 8.1 Hz, 1H), 7.64 – 7.53 (m, 3H), 7.50 (td, J = 7.5, 1.2 Hz, 2H), 7.41 (t, J = 7.4 Hz, 2H), 7.33 (t, J = 7.4 Hz, 1H), 2.46 (s, 3H).

Synthesis of 3-acetyl-7-hexylpyrano[*3,2-c*]carbazole-2(*7H*)-one (**CCK–Me**). **2a** (0.5 g, 1.80 mmol) was dissolved in dry DMF (20 mL) in a flask fitted with a magnetic stirrer and condenser. Then bromohexane (0.34 g, 1.80 mmol) and potassium carbonate (0.49 g, 3.60 mmol) were added. Then a small amount of potassium iodide and 18-crown-6 were added as catalyst. The reaction was heated at 100 °C for 24 h under N_2. The mixture was cooled to room temperature, the inorganic salt was filtered off and the precipitate was washed with DMF (2 × 30 mL). Then the filtrate was poured into sodium chloride aqueous solution (5 wt%, 500 mL). The gained precipitation was filtered off and then dissolved in dichloromethane, dried with Na_2SO_4 and concentrated under reduced pressure. The crude product was further purified by silica gel column chromatography (petroleum ether/ethyl acetate = 5:1) to get hold of **CCK–Me** in 59% yield. [^1]H NMR (400 MHz, DMSO-d_6): δ 8.80 (s, 1H), 8.30 (d, J = 7.7 Hz, 3H), 7.92 (d, J = 8.7 Hz, 1H), 7.76 (d, J = 8.3 Hz, 1H), 7.68 (d, J = 8.7 Hz, 1H), 7.57 (t, J = 8.3 Hz, 1H), 7.40 (t, J = 7.5 Hz, 1H), 4.47 (t, J = 7.1 Hz, 2H), 2.51 (p, J = 1.7 Hz, 6H), 1.78 (p, J = 7.1 Hz, 3H), 1.35 – 1.02 (m, 10H), 0.80 (t, J = 7.0 Hz, 3H). [^13]C NMR (101 MHz, DMSO–d_6): δ 195.14, 159.53, 152.43, 149.50, 144.78, 140.35, 128.59, 126.98, 122.73, 121.65, 120.50, 119.07, 110.98, 110.53, 108.81, 108.26, 43.35, 31.36, 30.63, 29.07, 26.44,

22.45, 14.29. Elemental Analysis (%) for $C_{23}H_{23}NO_3$: C, 76.43; H, 6.41; N, 3.88; O, 13.28.

Synthesis of 3-benzoyl-7-hexylpyrano[*3,2-c*]carbazole-2(*7H*)-one (**CCK–Ph**). A similar synthetic method as that described for **CCK–Me** was used to prepare **CCK–Ph**. The product was purified by column chromatography (petroleum ether/ethyl acetate = 5:1) to get hold of **CCK–Ph** in 55% yield. ^{1}H NMR (400 MHz, DMSO-d_6): δ 8.61 (s, 1H), 8.36 (d, J = 7.8 Hz, 1H), 7.94 (d, J = 7.3 Hz, 2H), 7.93 – 7.88 (m, 2H), 7.79 (d, J = 8.3 Hz, 1H), 7.73 (d, J = 8.6 Hz, 1H), 7.69 (t, J = 7.4 Hz, 1H), 7.62 – 7.51 (m, 4H), 7.41 (t, J = 7.5 Hz, 1H), 4.52 (t, J = 7.0 Hz, 2H), 1.92 – 1.68 (m, 3H), 1.37 – 1.10 (m, 9H), 0.80 (t, J = 7.0 Hz, 3H). ^{13}C NMR (101 MHz, DMSO-d_6): δ 195.70, 160.19, 155.06, 150.04, 143.79, 142.87, 138.61, 132.62, 129.98, 129.63, 129.02, 128.94, 128.76, 125.49, 124.01, 120.38, 112.43, 111.10, 110.32, 109.61, 107.37, 43.48, 31.37, 29.04, 26.43, 22.45, 19.30, 14.30. Elemental Analysis (%) for $C_{28}H_{25}NO_3$: C, 79.41; H, 5.95; N, 3.31; O, 11.33.

Synthesis of 7-hexyl-3-(2-methylbenzoyl)pyrano[*3,2-c*]carbazole-2(*7H*)-one (**CCK–Tol**). A similar synthetic method as that described for **CCK–Me** was used to prepare **CCK–Tol**. The product was purified by column chromatography (petroleum ether/ethyl acetate = 5:1) to get hold of **CCK–Tol** in 57% yield. ^{1}H NMR (400 MHz, DMSO-d_6): δ 8.60 (s, 1H), 8.30 (d, J = 7.7 Hz, 1H), 7.90 (d, J = 8.7 Hz, 1H), 7.74 (d, J = 8.3 Hz, 1H), 7.67 (d, J = 8.7 Hz, 1H), 7.61 – 7.51 (m, 3H), 7.45 (t, J = 7.5 Hz, 1H), 7.37 (q, J = 7.8 Hz, 3H), 7.28 (t, J = 7.5 Hz, 1H), 4.47 (t, J = 7.0 Hz, 2H), 2.51 (s, 1H), 1.98 – 1.57 (m, 3H), 1.42 – 1.00 (m, 13H), 0.78 (t, J = 7.0 Hz, 3H). ^{13}C NMR (101 MHz, DMSO-d_6): δ 197.46, 160.05, 154.86, 149.95, 143.75, 143.18, 139.69, 135.84, 131.25, 130.37, 129.95, 128.71, 128.18, 125.87, 125.12, 123.96, 120.62, 112.43, 111.12, 110.31, 109.59, 43.43, 31.34, 28.97, 26.41, 22.42, 19.87, 19.24, 14.26. Elemental Analysis (%) for $C_{29}H_{27}NO_3$: C, 79.61; H, 6.22; N, 3.20; O, 10.97.
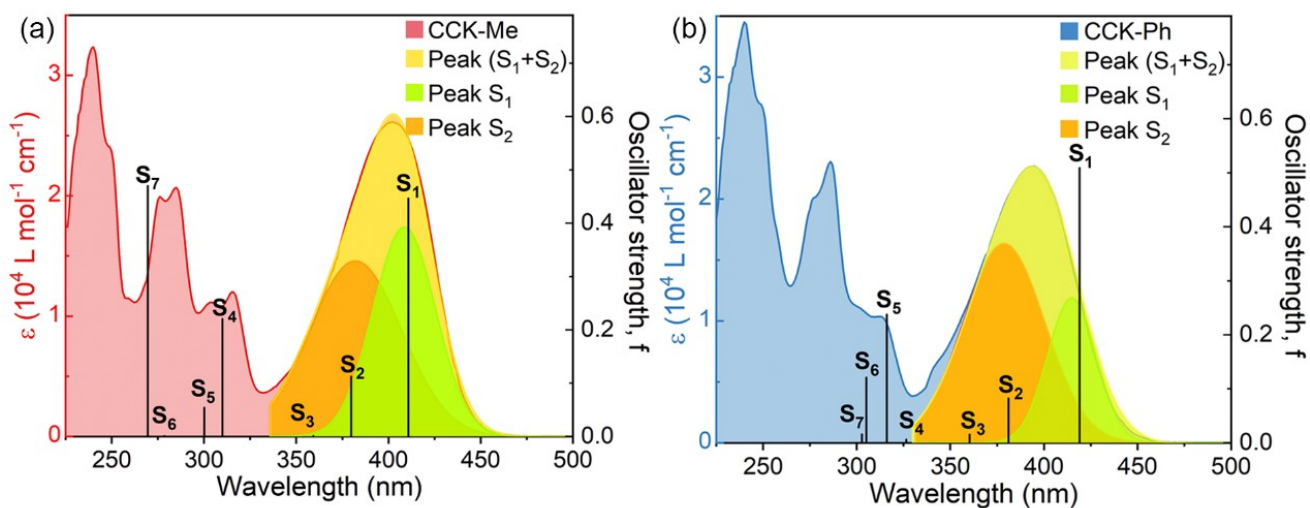
Fig. S1 The theoretical and experimental spectra of (a) CCK–Me and (b) CCK–Ph. S_1 (green area) and Peak S_2 (orange area) are obtained by fitting the peak–split of the lowest energy transition wavelengths obtained through theoretical calculation to the lowest energy absorption band of the experimental spectrum. Peak(S_1+S_2) (yellow area) is the sum of the two fitted peaks (green + orange).
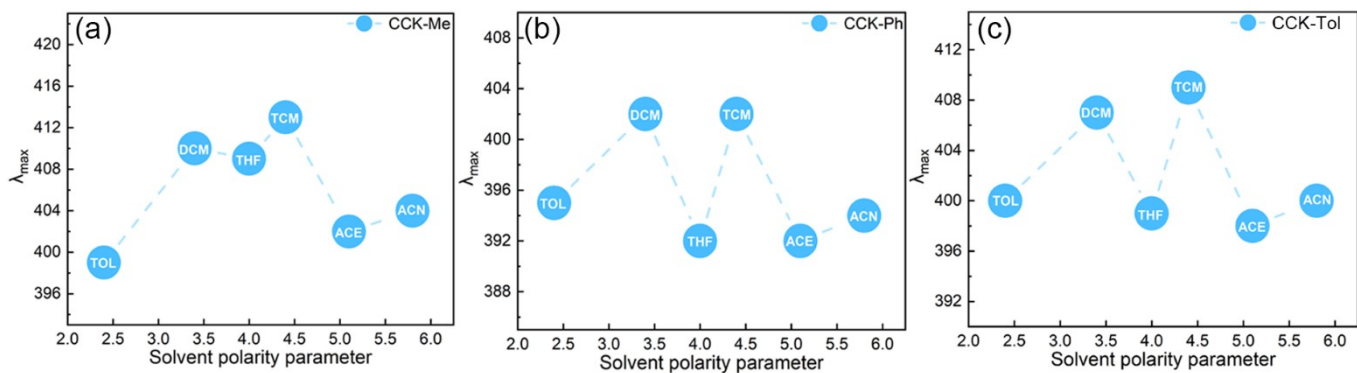
Fig. S2 Curves of absorption maximum wavelengths in different solvents versus solvent polarity parameters. (a) CCK–Me; (b) CCK–Ph; (c) CCK–Tol.
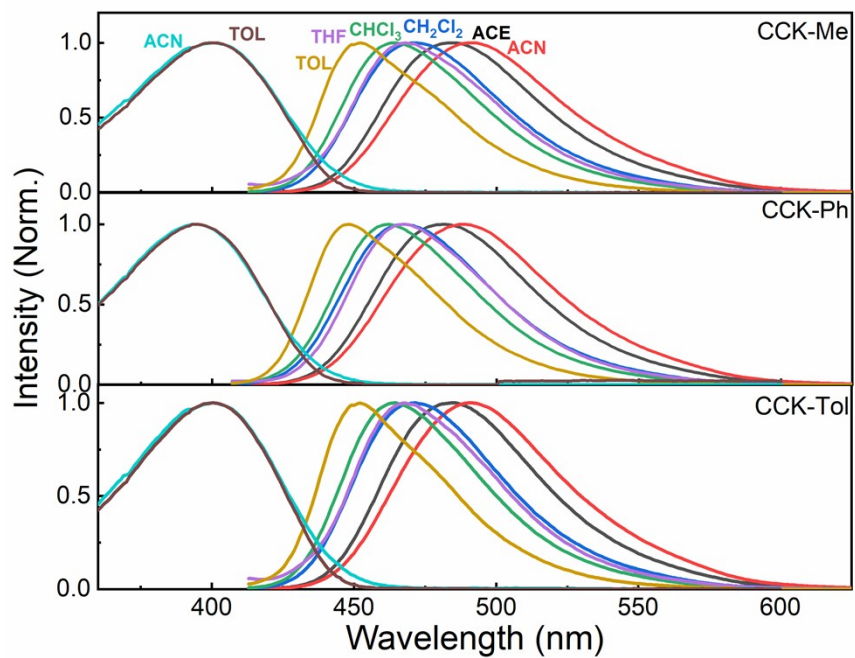
Fig. S3 Normalized absorption and fluorescence spectra of CCK–Me, CCK–Ph, and CCK–Tol in solvents of different polarity.
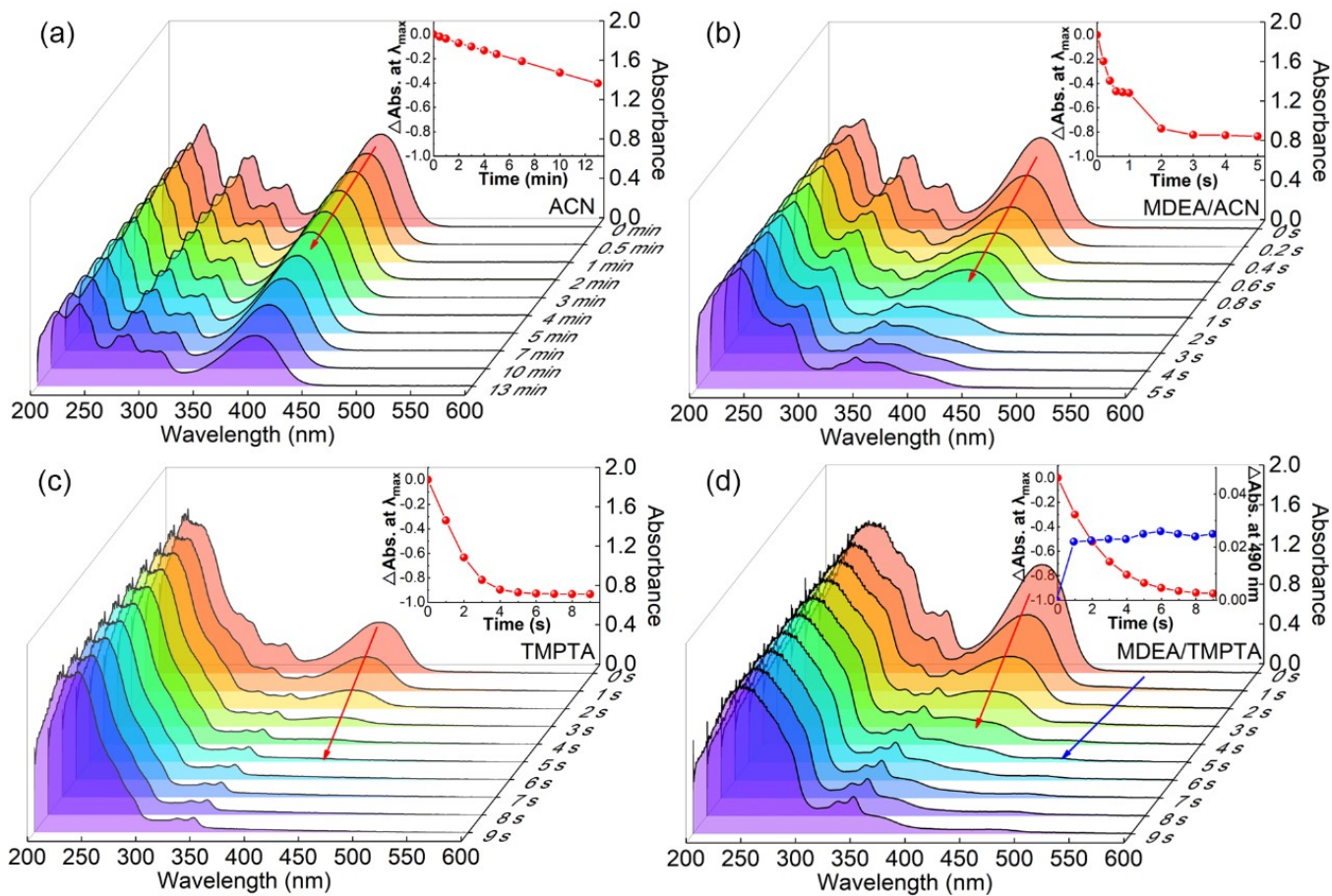
Fig. S4 UV–vis absorption spectra obtained upon photolysis of (a) CCK–Me in ACN, (b) CCK–Me/MDEA (1/2, n/n) in ACN, (c) CCK–Me in TMPTA, (d) CCK–Me/MDEA (0.5%/1%, wt/wt) in TMPTA upon irradiation at 405 nm. Inset: normalized absorbance at λ_{max} as a function of irradiation time. Light intensity: 45 mW cm^{-2}.
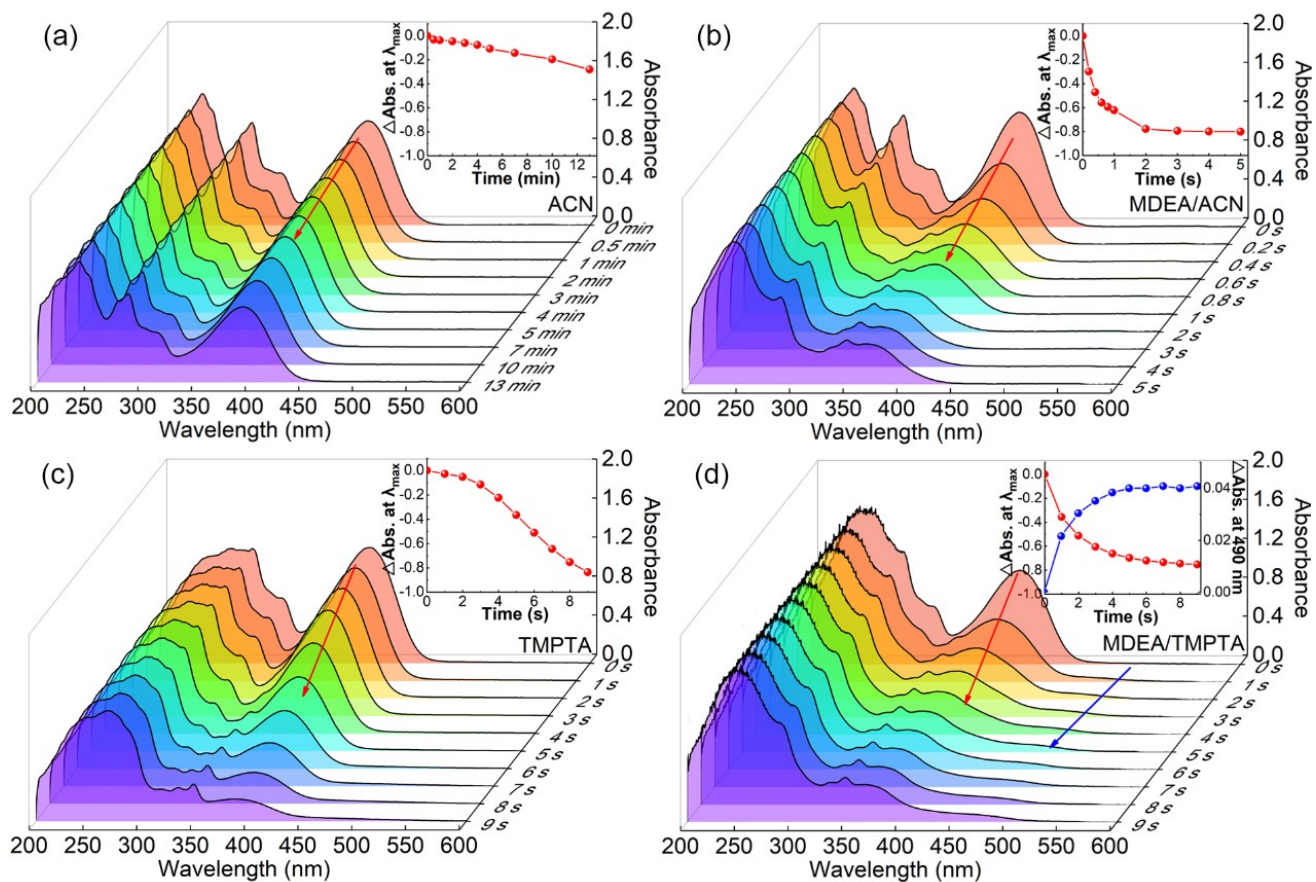
Fig. S5 UV–vis absorption spectra obtained upon photolysis of (a) CCK–Ph in ACN, (b) CCK–Ph/MDEA (1/2, n/n) in ACN, (c) CCK–Ph in TMPTA, (d) CCK–Ph/MDEA (0.5%/1%, wt/wt) in TMPTA upon irradiation at 405 nm. Inset: normalized absorbance at λ_{max} as a function of irradiation time. Light intensity: 45 mW cm^{-2}.
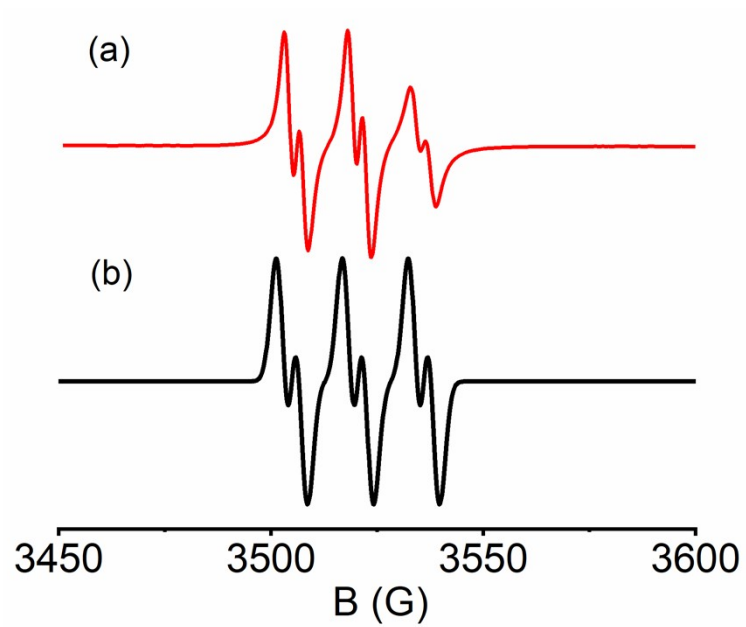
Fig. S6 ESR-ST spectra obtained after light irradiation of CCK–Tol/MDEA in *tert*-butylbenzene (PBN is used as a spin-trap reactant). (a) experimental and (b) simulated spectra.

Table S1 Hfc (hyperfine coupling constants) for the detected spin adduct of PBN in *tert*-butylbenzene of two PIs systems.

PIs systems	**Radical 1**	**Radical 2**
CCK–Tol	a_N=14.6 G, a_H=2.5 G; (88.89%)	a_N=14.9 G, a_H=2.5 G (11.11%)
CCK–Tol/MDEA	a_N=14.5 G; a_H=2.8 G	/

Table S2 Photopolymerization results of TMPTA in the presence of PIs/MDEA (0.5%/1.0% wt/wt) under irradiation by distinct LED sources at ca. 45.0 mW cm^{-2} and 405, 425, 450, and 475 nm as determined via photo-DSC.

PIs	LEDs	Heat flow (mW mg^{-1})	$R_p/[M]_{max}{}^a$ (s^{-1})	Conversion (%)
CCK–Me		35.06	2.29	44.14
CCK–Ph		29.24	1.91	44.60
CCK–Tol	405 nm	26.50	1.74	37.98
CQ		9.65	0.63	26.07
CCK–Me		35.14	2.30	44.11
CCK–Ph		38.41	2.52	55.09
CCK–Tol	425 nm	39.26	2.57	50.72
CQ		12.30	0.81	27.93
CCK–Me		33.14	2.17	49.70
CCK–Ph		31.93	2.09	51.60
CCK–Tol	450 nm	35.84	2.35	49.78
CQ		14.06	0.82	31.91
CCK–Me		27.46	1.80	45.42
CCK–Ph		25.97	1.70	42.85
CCK–Tol	475 nm	31.08	2.04	48.89

| CQ | | 14.00 | 0.92 | 31.55 |

[a] R_p/[M]: maximum of the first derivative of the conversion rate time profile.

¹H NMR (600 MHz, Chloroform-*d*) δ 12.42 (s, 1H), 9.88 (s, 1H),
8.37 (d, *J* = 7.7 Hz, 2H), 7.49 (d, *J* = 8.4 Hz, 1H), 7.45 (d, *J* = 3.8
Hz, 3H), 7.34 (dt, *J* = 8.0, 4.1 Hz, 1H), 7.01 (d, *J* = 8.4 Hz, 1H).
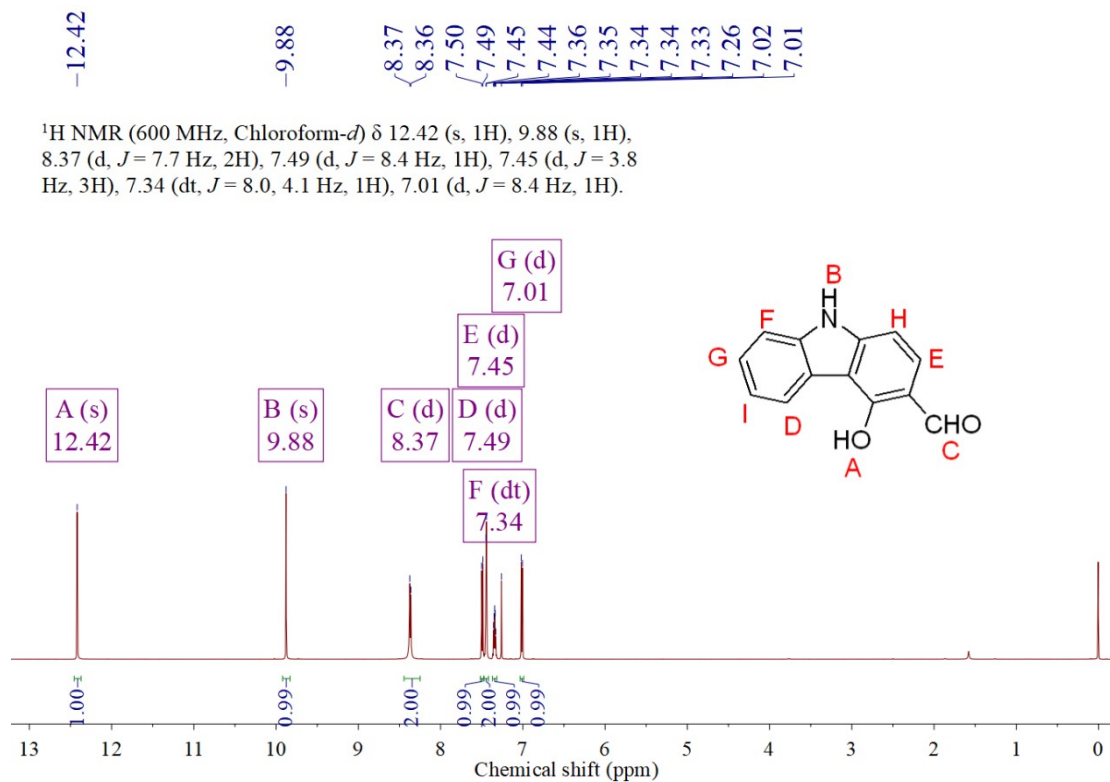
Fig. S7 ¹H-NMR spectrum of **1** in CDCl₃
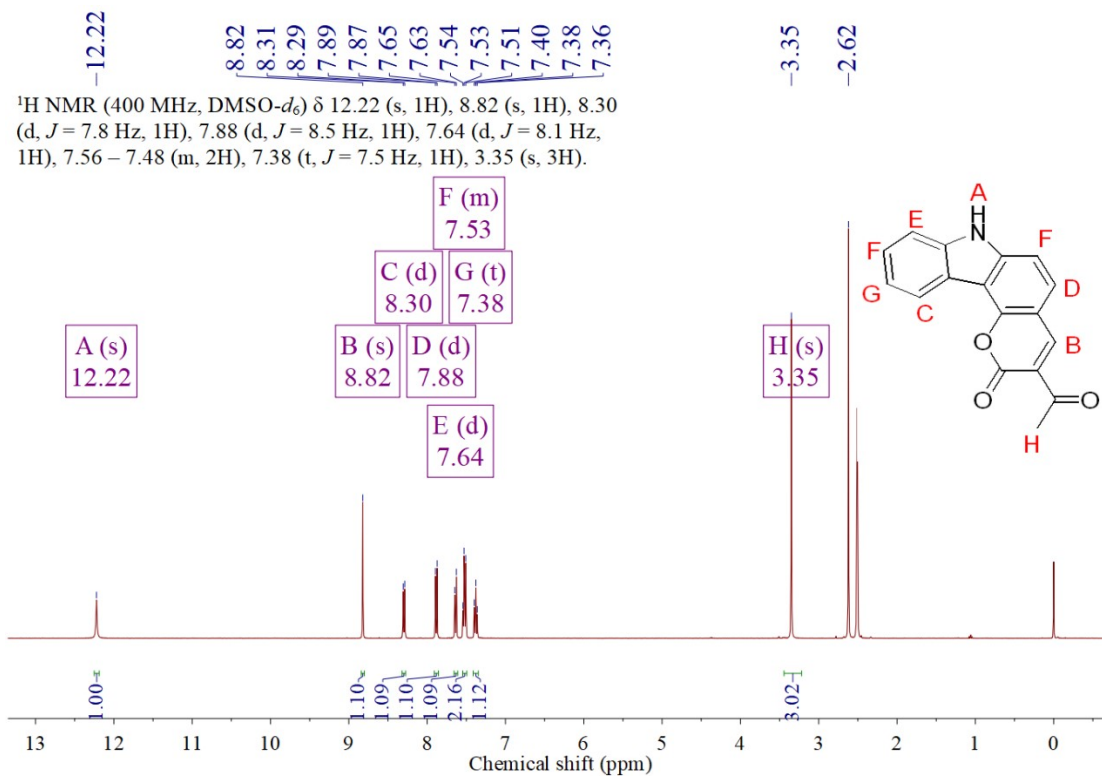
Fig. S8 ^{1}H-NMR spectrum of **2a** in DMSO-d_6

^{1}H NMR (400 MHz, DMSO-d_6) δ 12.22 (s, 1H), 8.82 (s, 1H), 8.30 (d, J = 7.8 Hz, 1H), 7.88 (d, J = 8.5 Hz, 1H), 7.64 (d, J = 8.1 Hz, 1H), 7.56 – 7.48 (m, 2H), 7.38 (t, J = 7.5 Hz, 1H), 3.35 (s, 3H).
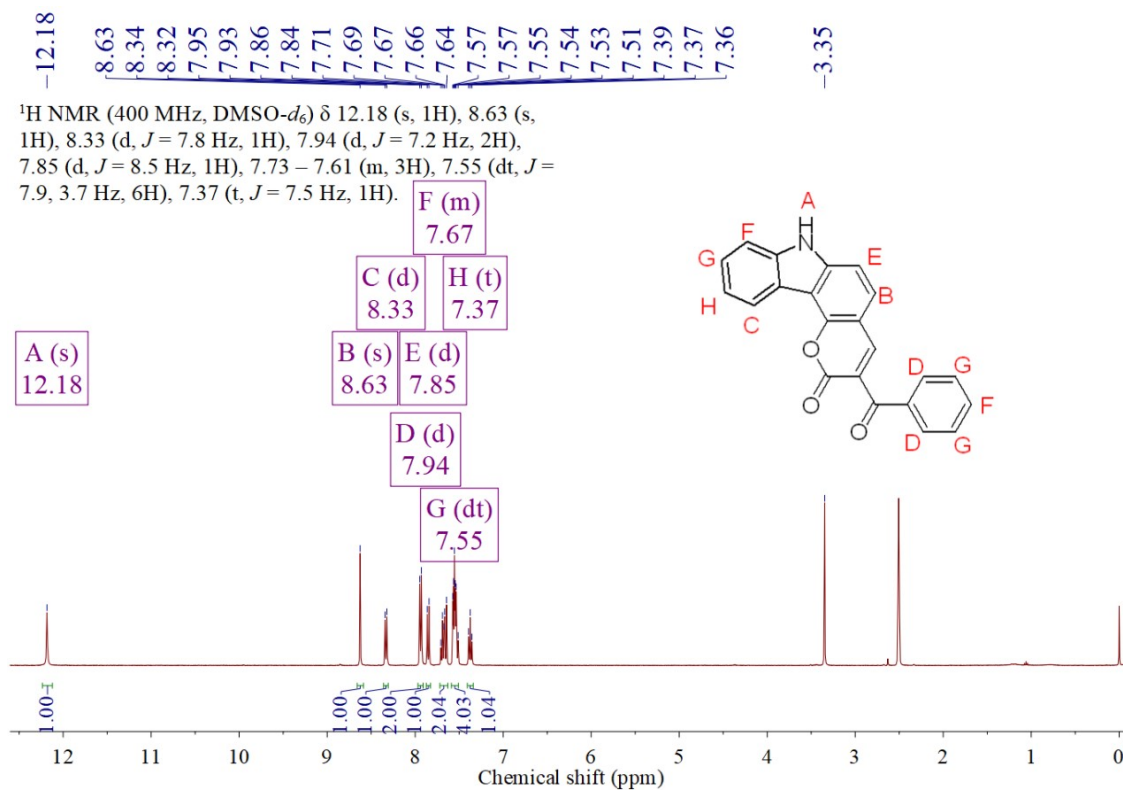
Fig. S9 ^{1}H-NMR spectrum of **2b** in DMSO-d_6

^{1}H NMR (400 MHz, DMSO-d_6) δ 12.18 (s, 1H), 8.63 (s, 1H), 8.33 (d, J = 7.8 Hz, 1H), 7.94 (d, J = 7.2 Hz, 2H), 7.85 (d, J = 8.5 Hz, 1H), 7.73 – 7.61 (m, 3H), 7.55 (dt, J = 7.9, 3.7 Hz, 6H), 7.37 (t, J = 7.5 Hz, 1H).

19
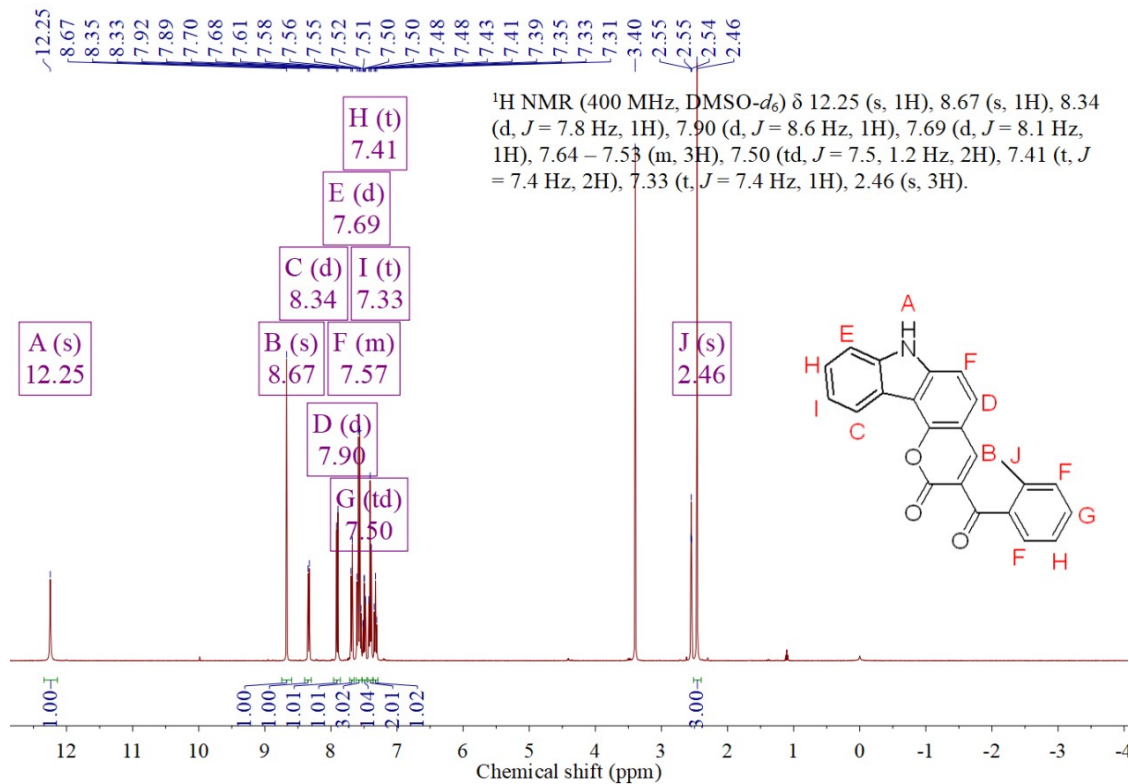
Fig. S10 ^{1}H-NMR spectrum of **2c** in DMSO-d_6

^{1}H NMR (400 MHz, DMSO-d_6) δ 12.25 (s, 1H), 8.67 (s, 1H), 8.34 (d, J = 7.8 Hz, 1H), 7.90 (d, J = 8.6 Hz, 1H), 7.69 (d, J = 8.1 Hz, 1H), 7.64 – 7.53 (m, 3H), 7.50 (td, J = 7.5, 1.2 Hz, 2H), 7.41 (t, J = 7.4 Hz, 2H), 7.33 (t, J = 7.4 Hz, 1H), 2.46 (s, 3H).
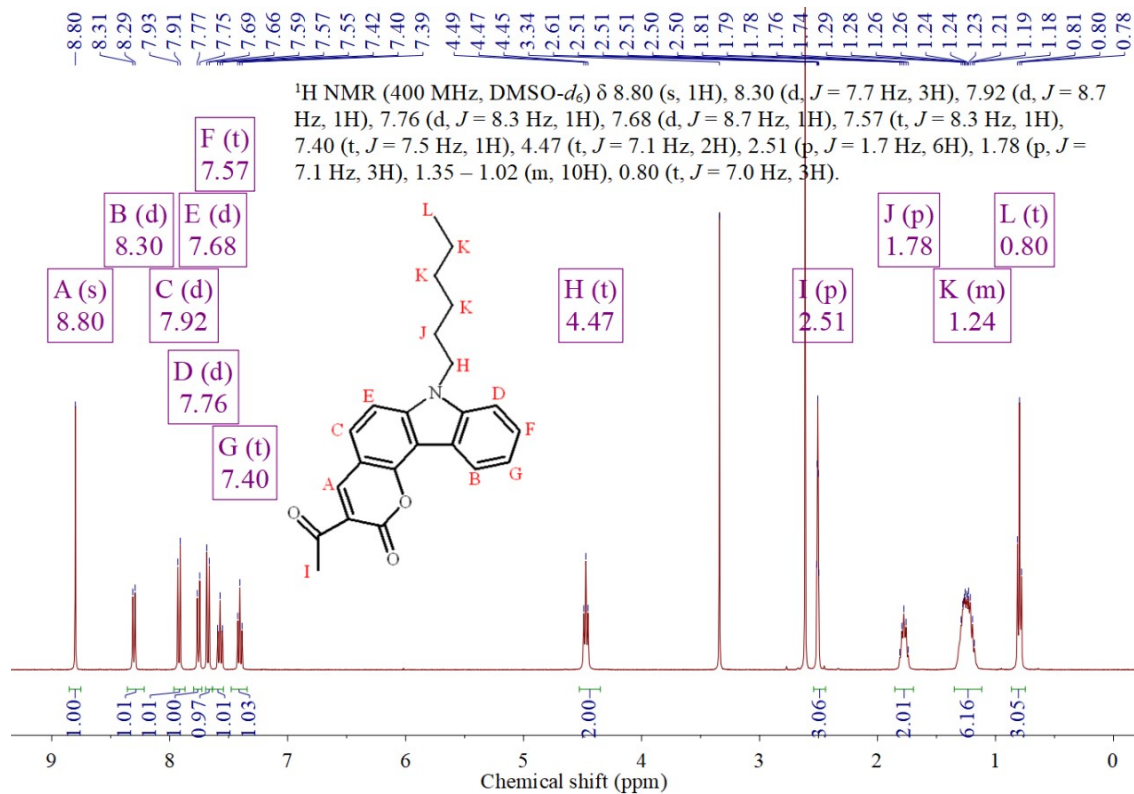
Fig. S11 ^{1}H-NMR spectrum of **CCK–Me** in DMSO-d_6

^{1}H NMR (400 MHz, DMSO-d_6) δ 8.80 (s, 1H), 8.30 (d, J = 7.7 Hz, 3H), 7.92 (d, J = 8.7 Hz, 1H), 7.76 (d, J = 8.3 Hz, 1H), 7.68 (d, J = 8.7 Hz, 1H), 7.57 (t, J = 8.3 Hz, 1H), 7.40 (t, J = 7.5 Hz, 1H), 4.47 (t, J = 7.1 Hz, 2H), 2.51 (p, J = 1.7 Hz, 6H), 1.78 (p, J = 7.1 Hz, 3H), 1.35 – 1.02 (m, 10H), 0.80 (t, J = 7.0 Hz, 3H).
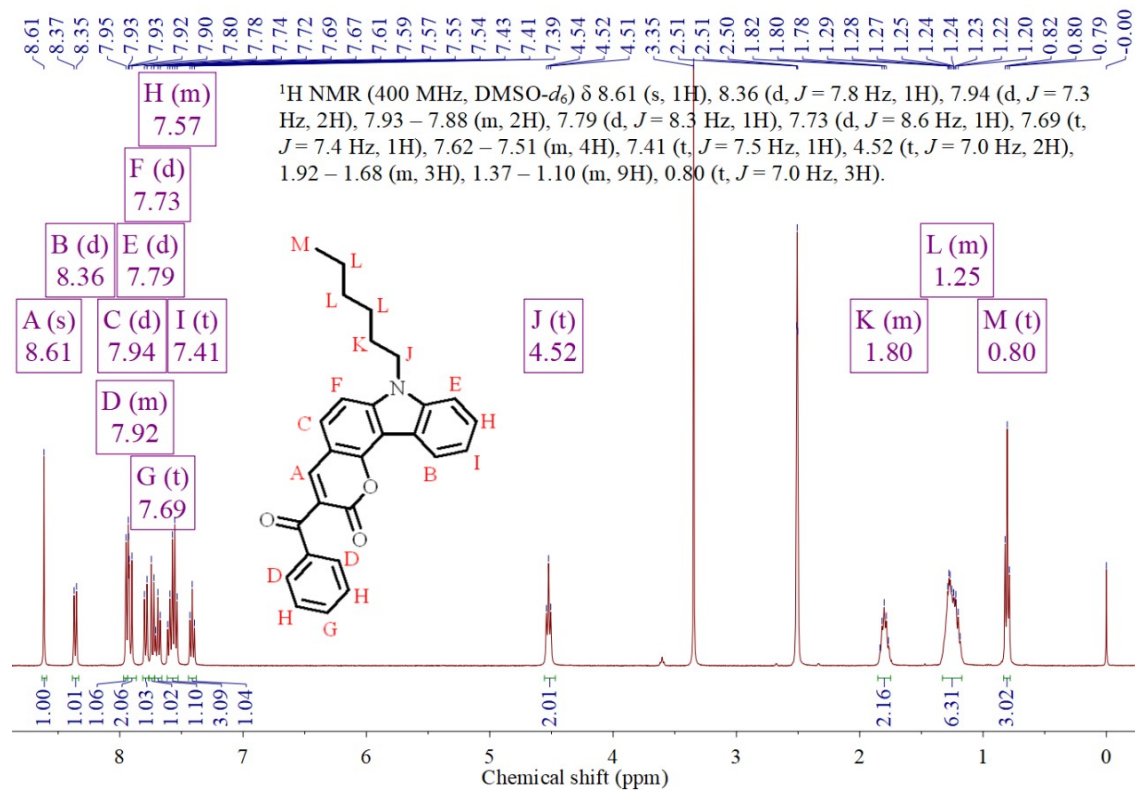
Fig. S12 ¹H-NMR spectrum of **CCK–Ph** in DMSO-d_6

¹H NMR (400 MHz, DMSO-d_6) δ 8.61 (s, 1H), 8.36 (d, J = 7.8 Hz, 1H), 7.94 (d, J = 7.3 Hz, 2H), 7.93 – 7.88 (m, 2H), 7.79 (d, J = 8.3 Hz, 1H), 7.73 (d, J = 8.6 Hz, 1H), 7.69 (t, J = 7.4 Hz, 1H), 7.62 – 7.51 (m, 4H), 7.41 (t, J = 7.5 Hz, 1H), 4.52 (t, J = 7.0 Hz, 2H), 1.92 – 1.68 (m, 3H), 1.37 – 1.10 (m, 9H), 0.80 (t, J = 7.0 Hz, 3H).
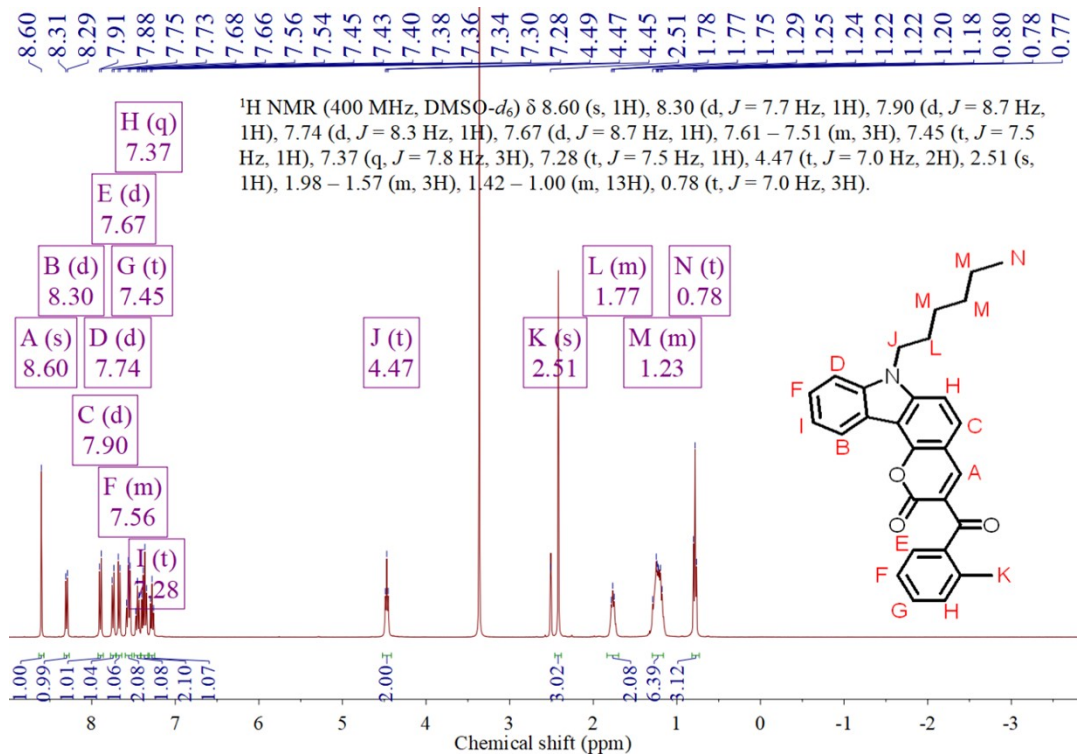
Fig. S13 ¹H-NMR spectrum of **CCK–Tol** in DMSO-d_6

¹H NMR (400 MHz, DMSO-d_6) δ 8.60 (s, 1H), 8.30 (d, J = 7.7 Hz, 1H), 7.90 (d, J = 8.7 Hz, 1H), 7.74 (d, J = 8.3 Hz, 1H), 7.67 (d, J = 8.7 Hz, 1H), 7.61 – 7.51 (m, 3H), 7.45 (t, J = 7.5 Hz, 1H), 7.37 (q, J = 7.8 Hz, 3H), 7.28 (t, J = 7.5 Hz, 1H), 4.47 (t, J = 7.0 Hz, 2H), 2.51 (s, 1H), 1.98 – 1.57 (m, 3H), 1.42 – 1.00 (m, 13H), 0.78 (t, J = 7.0 Hz, 3H).

^{13}C NMR (151 MHz, DMSO) δ 195.14, 159.53, 152.43, 149.50, 144.78, 140.35, 128.59, 126.98, 122.73, 121.65, 120.50, 119.07, 110.98, 110.53, 108.81, 108.26, 43.35, 31.36, 30.63, 29.07, 26.44, 22.45, 14.29.
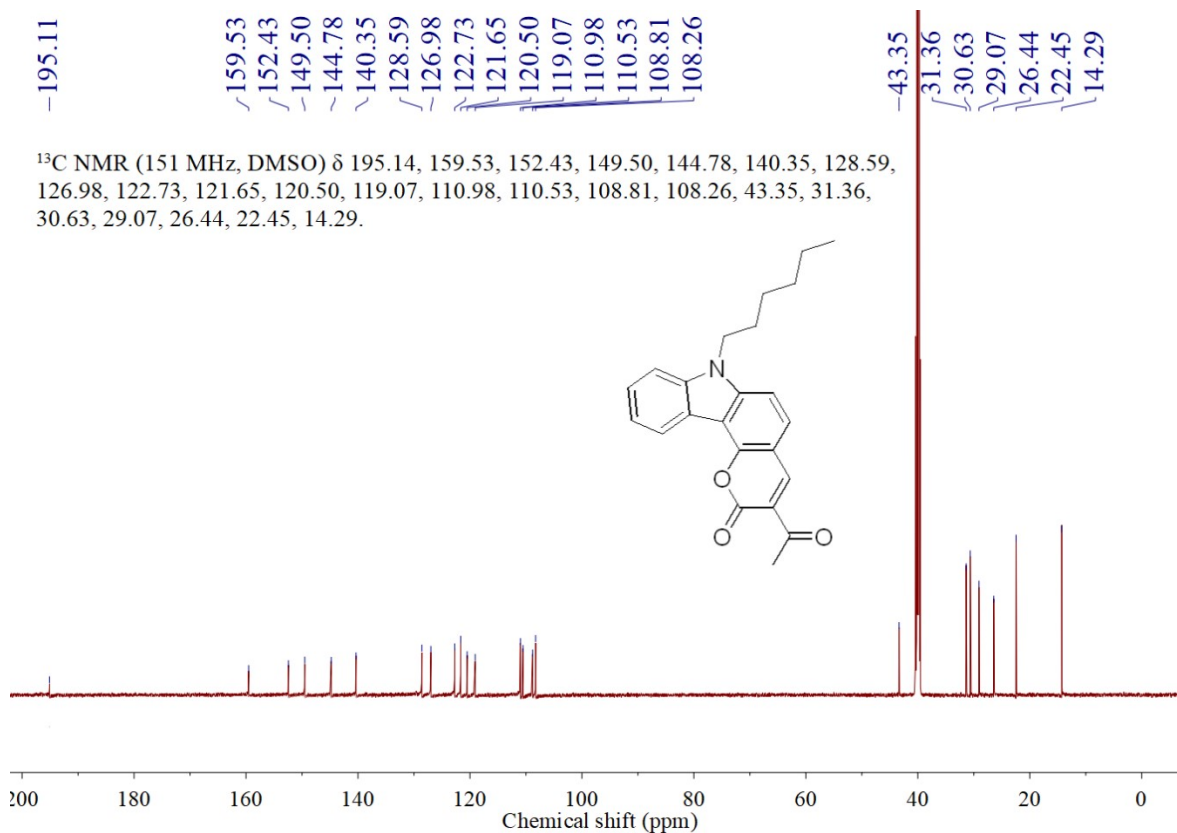
Fig. S14 ^{13}C-NMR spectrum of **CCK–Me** in DMSO-d_6

^{13}C NMR (151 MHz, DMSO) δ 195.70, 160.19, 155.06, 150.04, 143.79, 142.87, 138.61, 132.62, 129.98, 129.63, 129.02, 128.94, 128.76, 125.49, 124.01, 120.38, 112.43, 111.10, 110.32, 109.61, 107.37, 43.48, 31.37, 29.04, 26.43, 22.45, 19.30, 14.30.
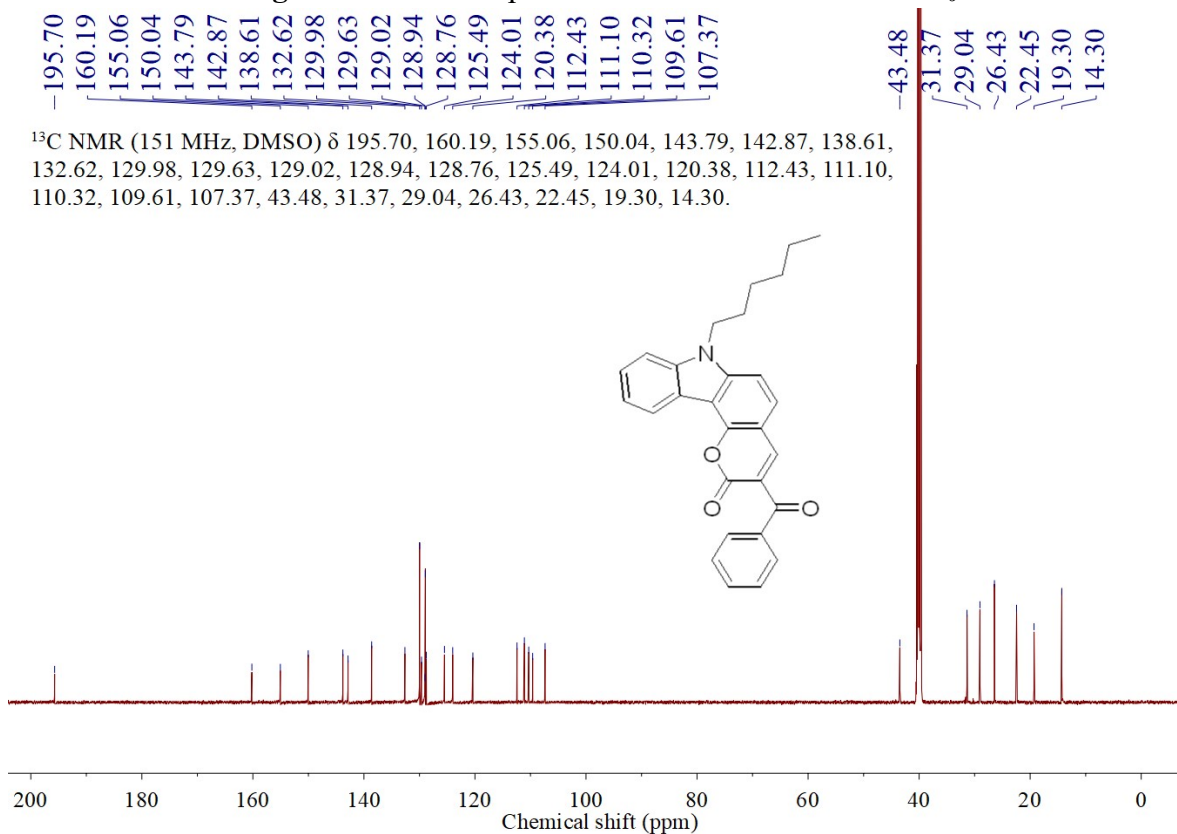
Fig. S15 ^{1}H-NMR spectrum of **CCK–Ph** in DMSO-d_6

^{13}C NMR (151 MHz, DMSO) δ 197.46, 160.05, 154.86, 149.95, 143.75, 143.18, 139.69, 135.84, 131.25, 130.37, 129.95, 128.71, 128.18, 125.87, 125.12, 123.96, 120.62, 112.43, 111.12, 110.31, 109.59, 43.43, 31.34, 28.97, 26.41, 22.42, 19.87, 19.24, 14.26.

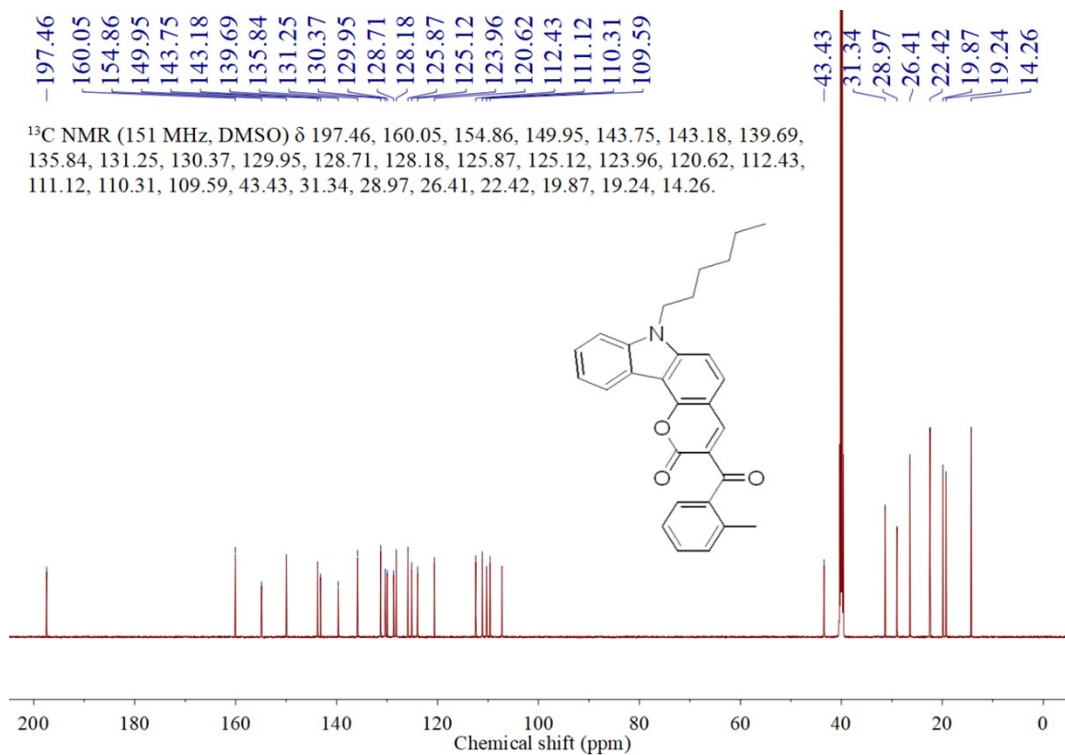**Fig. S16** ^{13}C-NMR spectrum of **CCK–Tol** in DMSO-d_6

Reference

1. R. Xia, J.-P. Malval, M. Jin, A. Spangenberg, D. Wan, H. Pu, T. Vergote, F. Morlet-Savary, H. Chaumeil, P. Baldeck, O. Poizat and O. Soppera, *Chem. Mater.*, 2012, **24**, 237-244.

2. A. Criqui, J. Lalevee, X. Allonas and J.-P. Fouassier, *Macromol. Chem. Phys.*, 2008, **209**, 2223-2231.

3. J. Wei and F. Liu, *Macromolecules*, 2009, **42**, 5486-5491.

4. M. Mitterbauer, P. Knaack, S. Naumov, M. Markovic, A. Ovsianikov, N. Moszner and R. Liska, *Angew. Chem., Int. Ed.*, 2018, **57**, 12146-12150.